Journal of Inflammation Research

Dovepress
Taylor & Francis Group

Open Access Full Text Article

ORIGINAL RESEARCH

Calycosin-7-Glucoside Alleviates Atherosclerosis by Inhibiting Ox-LDL-Induced Foam Cell Formation and Inflammatory Response in THP-1-Derived Macrophages via ATF-1 Activation Through the p38/MAPK Pathway

Rui Chen[1,*], Jiaqian Fang[2,*], Hairuo Sun[3,*], Zhiyong Yu[4,*], Yangfan Huang[2], Yaohong Song[1]

[1]Department of Cardiology, Nanjing Hospital of Chinese Medicine Affiliated to Nanjing University of Chinese Medicine, Nanjing, People's Republic of China; [2]Nanjing University of Chinese Medicine, Nanjing, People's Republic of China; [3]College of Chemistry and Chemical Engineering, China University of Petroleum (East China), Qingdao, People's Republic of China; [4]Department of Cardiology, Taihe County People's Hospital, Fuyang, People's Republic of China

*These authors contributed equally to this work

Correspondence: Yaohong Song, Department of Cardiology, Nanjing Hospital of Chinese Medicine Affiliated to Nanjing University of Chinese Medicine, Nanjing, People's Republic of China, Email sfy003@njucm.edu.cn

Purpose: Macrophages play a pivotal role in the progression of atherosclerosis (AS), and targeting macrophage-associated pathological processes has emerged as a promising therapeutic strategy for AS. Flavonoids have demonstrated potent antioxidant properties with potential anti-atherosclerotic effects. This study aimed to investigate the therapeutic effects of the flavonoid calycosin-7-glucoside (CG) on AS and elucidate its underlying molecular mechanisms.

Methods: Macrophages were differentiated from human monocytic THP-1 cells by treatment with phorbol-12-myristate-13-acetate (PMA). Foam cell formation was induced by exposing differentiated macrophages to oxidized low-density lipoprotein (ox-LDL). Protein and inflammatory cytokine expression levels were assessed using RT-qPCR, Western blot, and ELISA assays. Total cholesterol and free cholesterol levels were quantified using commercial kits, and lipid droplet accumulation was visualized using Nile red staining.

Results: Activation of activating transcription factor 1 (ATF-1) was found to mediate CG-induced suppression of inflammatory responses and foam cell formation in ox-LDL-exposed THP-1-derived macrophages. CG treatment enhanced p38 MAPK activity, which was responsible for ATF-1 activation and subsequent inhibition of inflammation and foam cell formation. Mechanistically, ATF-1 facilitated CG-induced anti-atherosclerotic effects by upregulating liver X receptor beta (LXR-β) and cystic fibrosis transmembrane conductance regulator (CFTR), which are critical for lipid metabolism and inflammation regulation, respectively.

Conclusion: CG attenuates ox-LDL-induced foam cell formation and inflammatory responses in THP-1-derived macrophages by activating the p38 MAPK/ATF-1 signaling pathway, leading to the upregulation of LXR-β and CFTR. These findings highlight the potential of CG as a therapeutic agent for AS.

Keywords: calycosin-7-glucoside, macrophage, foam cell formation, inflammatory response

Introduction

Atherosclerosis (AS) serves as the principal pathological driver of cardiovascular and cerebrovascular diseases, accounting for significant global morbidity and mortality.[1,2] Central to AS pathogenesis is the formation of lipid-laden foam cells, a process primarily mediated by oxidized low-density lipoprotein (ox-LDL) uptake in macrophages.[1,2] This pathogenic cascade triggers intracellular cholesterol accumulation, foam cell differentiation, and subsequent plaque formation and vascular remodeling. Given the pivotal role of ox-LDL-induced foam cell generation in AS progression,

Received: 26 January 2025
Accepted: 16 April 2025
Published: 25 April 2025

therapeutic strategies targeting this process hold considerable promise for preventing and potentially reversing atherosclerotic lesion development.[2]

Calycosin-7-glucoside (CG), a principal bioactive isoflavone derived from *Astragalus membranaceus*, exhibits diverse pharmacological properties including, neuroprotective effects, cardioprotective activity against myocardial injury, anticancer potential, and hepatic steatosis amelioration.[3–5] Notably, as a key serum component of Buyang Huanwu decoction, a traditional Chinese medicine formulation for cardiovascular and cerebrovascular disorders, CG has demonstrated antiatherosclerotic potential by inhibiting excessive mitochondrial fission in diabetic conditions.[6] Despite these promising findings, the therapeutic efficacy of CG against AS and its precise molecular mechanisms remain to be fully elucidated.

Activating transcription factor-1 (ATF-1), a member of the ATF/CREB family, functions as a crucial transcriptional regulator through its ability to form homo- or heterodimers with other bZIP transcription factors.[7] This versatile regulatory capacity enables ATF-1 to modulate the expression of numerous target genes involved in diverse cellular processes, including, cell proliferation and differentiation, cellular survival and stress responses, and metabolic regulation.[7–10] Of particular therapeutic relevance, emerging evidence suggests that ATF-1-mediated pathways may confer protection against foam cell formation and oxidative stress in AS.[11] However, the precise molecular mechanisms by which ATF-1 regulates foam cell development and progression remain poorly understood, representing a critical knowledge gap in the field.

The p38 mitogen-activated protein kinase (MAPK) signaling pathway plays a pivotal role in AS pathogenesis by modulating foam cell formation and inflammatory responses.[12] While ATF-1 has been established as a downstream effector of p38 MAPK in various cell types, including macrophages,[9,13] its specific involvement in p38 MAPK-mediated regulation of foam cell formation and inflammatory responses remains to be elucidated. This knowledge gap presents an important area for investigation, given the therapeutic potential of targeting this signaling axis in AS.

Building upon these findings, the present study was designed to systematically investigate the therapeutic potential of CG in attenuating ox-LDL-induced foam cell formation and inflammatory responses, and the underlying molecular mechanisms in monocyte-derived macrophages.

Materials and Methods

Cell Culture and Differentiation

Human monocytic THP-1 cell lines were obtained from Shanghai Zhong Qiao Xin Zhou Biotechnology Co., Ltd (ZQ0086, Shanghai, China). Cells were maintained in RPMI1640 medium (ZQ-200, Zhong Qiao Xin Zhou) supplemented with 10% fetal bovine serum (ZQ0500, Zhong Qiao Xin Zhou) and incubated at 37 °C in a cell culture incubator containing 5% CO_2 and 95% air. THP-1 cells were differentiated into macrophages by incubating with 100 ng/mL phorbol-12-myristate-13-acetate (PMA, HY-18739, MedChemExpress, USA) for 48 h. To induce foam cell formation, the harvested macrophages were cultured in serum-free medium containing 100 ng/mL ox-LDL (HY-NP013, MedChemExpress) for 24 h.

Cell Counting Kit 8 Assays

Cells were treated as indicated, the cell counting kit-8 (CCK-8; HY-K0301, MedChemExpress) reagent was subsequently added in the culture medium and the cells were then incubated for 1 h. The microplate reader (Thermo Fisher Scientific) was used to measure the absorbance at 450 nm.

Western Blot Analysis

Western blot analysis was performed as described previously.[14] Briefly, a total of 25 ug proteins were separated using 4–12% SDS-PAGE gels and transferred onto PVDF membranes. The membranes were blocked with 5% skim milk at room temperature for 1 h, incubated with primary antibodies against NLRP3 (RM4624; 1μg/mL), ASC (BD-PT0365; 1μg/mL), caspase-1 (RM6624; 0.5μg/mL), ATF-1 (RM4830; 0.5μg/mL), Phospho-ATF-1 (BD-PT1351; 1μg/mL), CFTR (BD-PT0888; 0.5μg/mL), ERK (BD-PT1625; 0.5μg/mL), Phospho-ERK (BD-PP0101; 1μg/mL), AKT (RM1117; 0.5μg/mL), Phospho-AKT (RM4971; 1μg/mL), JNK (RM1210; 0.5μg/mL), Phospho-JNK (RM2676;1μg/mL), p38 (RM4573; 0.5μg/mL), Phospho-p38 (RM2014; 1μg/mL), ABCA1 (BD-PN2847; 0.5μg/mL), and β-actin (B8010; 0.25μg/mL) at 4 °C overnight, followed by corresponding secondary antibodies. All primary and secondary antibodies were obtained from

Biodragon (Suzhou, China). Blots were developed by ECL detection reagents (PECL08, Proteinbio, China). The Gel-Pro image program (Media Cybernetics, Las Vegas, USA) was used to measure the intensities of the bands.

Enzyme-Linked Immunosorbent Assay (ELISA)

The levels of pro-inflammatory cytokines (TNF-α, IL-1β, and IL-6) and anti-inflammatory cytokines (IL-10) in cell culture medium were determined using the following ELISA kits: TNF-α ELISA Kit (NOV-FM-E100136; Neobioscience, China), IL-10 ELISA Kit (NOV-NB-E10155; Neobioscience), IL-6 ELISA Kit (EHC007; Neobioscience), and IL-1β ELISA Kit (NOV-FM-E100053; Neobioscience). Procedures were conducted according to the manufacturer's instructions.

Nile Red Staining

Nile red staining was used to analyze the lipid droplet content in differentiated THP-1 cells. Briefly, THP-1 cells were treated with ox-LDL as indicated and then stained with 1 μM Nile red (HY-D0718, MCE) in the dark for 10 min. The fluorescence microscope (Leica DM2500, Wetzlar, Germany) was used to observe the stained cells.

Cellular Cholesterol Efflux

Cells were treated as indicated and then washed twice with PBS. The cells were subsequently labeled with DMEM containing [3H]-cholesterol (0.5 μCi/mL, catalog no. NET139001MC; PerkinElmer) and 0.1% (w/v) fatty acid–free bovine serum albumin for 24 h. The liquid scintillation counting method was employed to detect the medium and cell-associated [3H]-cholesterol. The percentage of efflux was calculated using the following formula: [total media counts/(total cellular counts + total media counts)] × 100%.

Measurement of Free Cholesterol and Total Cholesterol

The levels of free cholesterol (FC) and total cholesterol (TC) in the culture medium were measured by commercial kits (E1005 for TC; E1016 for FC; Applygen Technologies Inc., Beijing, China) following the manufacturer's instructions.

Transfection of Small Interfering RNAs

FAM-labeled siRNAs against ATF-1, LXR-β, and CFTR were obtained from GenePharma Co Ltd (Shanghai, China). The siRNAs were transfected into cells with Lipofectamine^{TM} RNAiMAX transfection reagents (13778150, Thermo Fisher Scientific, USA) according to the manufacturer's protocol at a final concentration of 50 nM. Transfection efficiency was proved by fluorescence microscope and target gene knockdown was validated using Western blot. The sequences of control siRNAs and the siRNA against ATF-1, LXR-β, and CFTR were as follows: ATF-1, Forward, 5′-UUCUGAUAAAGAUGAUACCUG-3′, Reverse, 5′-UUCUGAUAAAGAUGAUACCUG-3′; LXR-β, Forward, 5′-UUUACAGUGGGUGAAGAAGAA-3′, Reverse, 5′-CUUCUUCACCCACUGUAAAGG-3′; CFTR, Forward, 5′-UAUCCUUUCCUCAAAAUUGGU-3′, Reverse, 5′-CAAUUUUGAGGAAAGGAUACA-3′.

Chromatin Immunoprecipitation (ChIP) Assay

The binding relationship between ATF-1 and LXR-β or CFTR was validated by using a chromatin immunoprecipitation (ChIP) assay kit (Cat. No. P2078, Beyotime, Shanghai, China). Briefly, after treatment as described in the text, cells were cross-linked with 1% formaldehyde for 10 min. The reaction was quenched with glycine (0.125 mol/L) for 5 min. Cells were then washed with ice-cold 1× PBS and resuspended in lysis buffer for ultrasonic treatment four times (model 550 sonic dismembrane; Fisher). The A/G agarose magnetic beads were conjugated with 4 μg anti-ATF-1 (RM4830, Biodragon) or anti-IgG (Cat. No. A7016, Beyotime) and then incubated with the cell lysate overnight at 4 °C. Cross-links was reversed at 65 °C for 4 h, and then DNA was recovered by phenol/chloroform extraction. LXR-β or CFTR promoter enrichment was determined by qPCR. The following primer sequences were used: LXR-β, 5′-TCCAACTTCCGTGCGGGGCA-3 and 5′-CGTCCGGAAGAGGGGCGGAG-3′; CFTR, 5′-GGGCAGTGAAGGCGGGGGAAAGAGC-3′ and 5′-CTGGGTGCCTGCCGCTCAACCCTT-3′.

https://doi.org/10.2147/JIR.S516160

Quantitative Real-Time Reverse Transcription Polymerase Chain Reaction (qRT-PCR)

Total RNA was extracted from cells using Trizol reagent (15596018CN; Thermo fisher scientific) following the manufacturer's instructions, and 1 μg of total RNA was reverse transcribed into cDNA using One Step PrimeScript miRNA cDNA Synthesis kit (#D350A; TaKaRa, Dalian, China). Real-time PCR assays were carried out using TB Green Premix Ex *Taq* II (RR820A) on an ABI 7300 Real-Time PCR System (Applied Biosystem, Foster City, USA). The gene expression levels were calculated using the $2^{-\Delta\Delta CT}$ method, and GAPDH was used as the internal control. The following primers were used: LXR-β-forward, 5′-AACAACTGGGCATGATCGAG-3′ and LXR-β-reverse, 5′-CTCAGTGAAGTGGGCAAAGC-3′; CFTR-forward, 5′- GCTCCTACACCCAGCCATTT-3′ and CFTR-reverse, 5′- AGAACACGGCTTGACAGCTT-3′; and *GAPDH*-forward, 5′- CTGACTTCAACAGCGACACC-3′ and *GAPDH*-reverse, 5′- GTGGTCCAGGGGTCTTACTC-3′.

Statistical Analysis

Data are expressed as mean ± standard deviation (SD) from a minimum of three independent experiments. All statistical analyses were conducted using Prism 10.0 software (GraphPad Software, San Diego, CA, USA). Prior to analysis, data were assessed for normality (Shapiro–Wilk test) and homogeneity of variance (Levene's test). For datasets satisfying these assumptions, comparisons between two groups were performed using Student's *t*-test, while multiple-group comparisons were analyzed by ordinary one-way ANOVA followed by Bonferroni and Tamhane's T2 post-hoc tests. For datasets violating normality or homogeneity assumptions, non-parametric tests were applied. A P-value < 0.05 was considered statistically significant.

Results

CG Increases the Viability of THP-1-Derived Macrophage

To determine the effect of CG on the viability of THP-1-derived macrophage, THP-1 cells were induced to differentiate into macrophages by PMA treatment (100 nM) for 48 h. As shown in Figure 1A, cell viability remains unchanged with CG treatment (0–100 μM), suggesting that CG had no cytotoxic effect on THP-1-derived macrophage. To assess CG′s protective effect on ox-LDL-induced foam cells and inflammation, THP-1-derived macrophage were pretreated with different concentrations of CG for 24 h prior to being stimulated with 50 μg/mL ox-LDL. As shown in Figure 1B, CG reduced ox-LDL-caused cell viability damage in THP-1-derived macrophage in a dose-dependent manner. As CG at 30 μM showed the best improvement on cell viability, it was selected as the optimal dose in subsequent experiments.

CG Suppresses Ox-LDL-Induced Inflammation in THP-1-Derived Macrophage

To determine the effect of CG on ox-LDL-induced inflammation, the production of inflammatory cytokines was detected. As shown in Figure 2A–D, ox-LDL induced excessive production of pro-inflammatory cytokines (TNF-α, IL-1β, and IL-6) and decreased the production of anti-inflammatory cytokines (IL-10). CG treatment decreased the production of pro-inflammatory

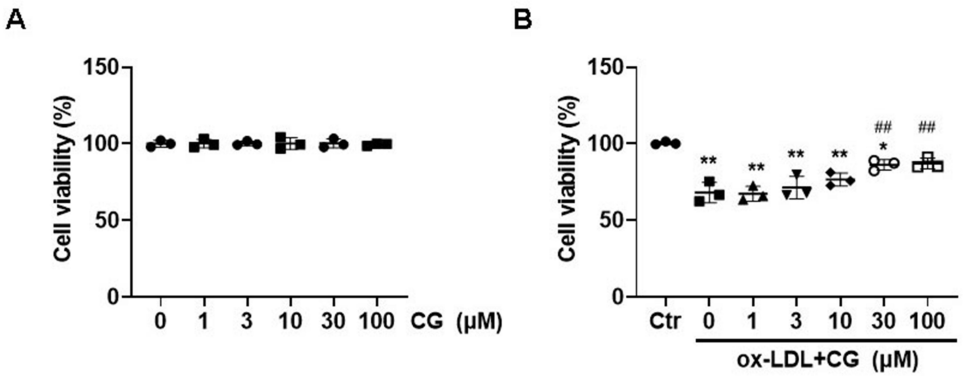

Figure 1 Effect of CG on the viability of THP-1-derived macrophage. (**A**) THP-1-derived macrophage were incubated with CG at different concentrations (0, 1, 3, 10, 30, and 100 μM) for 48 h, and the cell viability was detected using CCK-8 assay. (**B**) THP-1-derived macrophage cells were incubated with CG (0, 1, 3, 10, 30, and 100 μM) for 24 h, prior to being stimulated with ox-LDL (50 μg/mL) for 24 h. Then, the cell viability was detected using CCK-8 assay. *p<0.05, **p<0.01 compared with control (Ctr) group; ##p<0.01 compared with ox-LDL group.

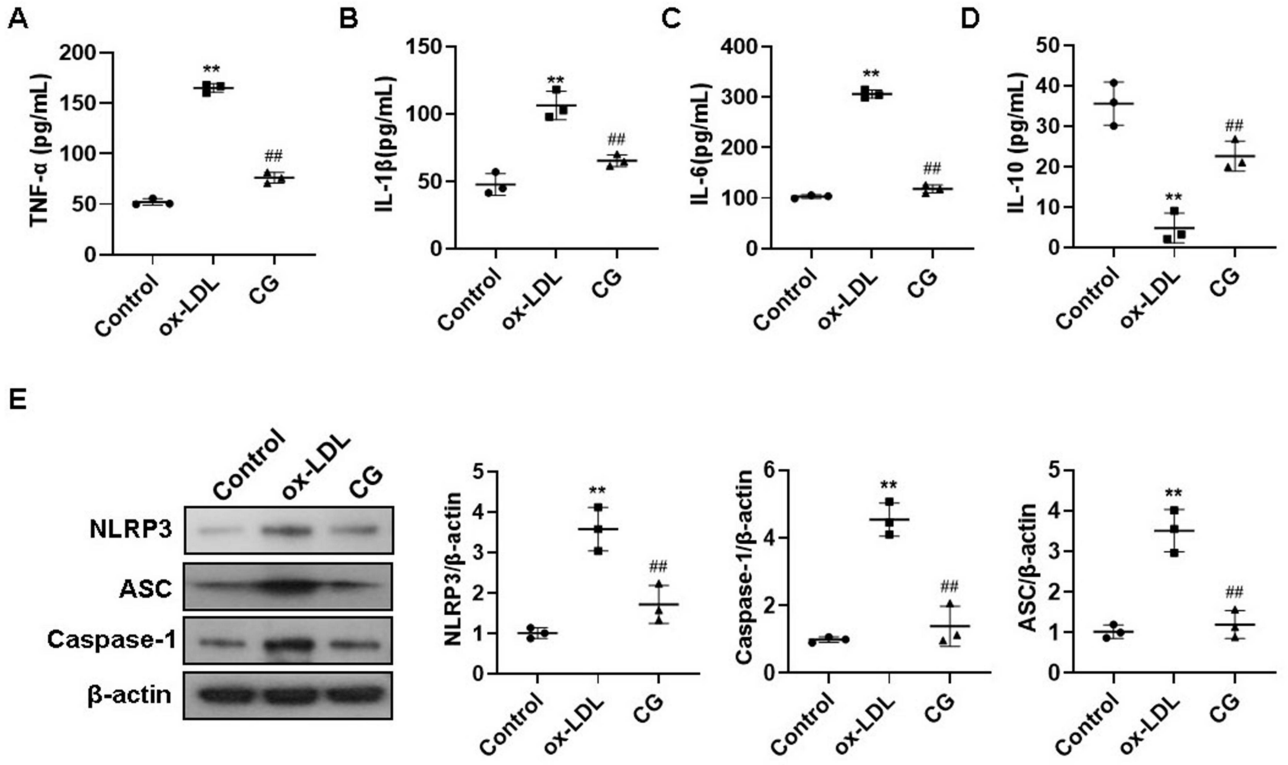

Figure 2 The effect of CG on ox-LDL-induced inflammation in THP-1-derived macrophage. THP-1-derived macrophage were incubated with CG for 24 h, prior to being stimulated with ox-LDL for 24 h. The production of inflammatory cytokines, including IL-6, IL-1β, TNF-α, and IL-10, was assayed by ELISA kits (**A**–**D**). **p<0.01 compared with control group; ##p<0.01 compared with ox-LDL group.

cytokines and increased the production of anti-inflammatory cytokines. Furthermore, the expression levels of NLRP3 inflammasome-related proteins (NLRP3, ASC, and Caspase-1) were obviously increased upon ox-LDL exposure. However, the elevated expression levels of NLRP3 inflammasome-related proteins significantly decreased after CG treatment (Figure 2E). These results suggested that CG could inhibit ox-LDL-induced inflammation in THP-1-derived macrophage.

CG Suppresses Ox-LDL-Induced Foam Cell Formation in THP-1-Derived Macrophage

To investigate effect of CG on the formation of atherosclerotic foam cells, THP-1-derived foam cells were induced with ox-LDL. Nile red staining showed that the number of foam cells were increased after ox-LDL exposure, and CG pretreatment significantly decreased the number of foam cells (Figure 3A). Ox-LDL exposure significantly increased the levels of total cholesterol (TC) and free cholesterol (FC), which were then obviously reduced by CG treatment (Figure 3B). In addition, ox-LDL exposure could reduce the percentage of cellular cholesterol efflux, while CG treatment ameliorated the decrease induced by ox-LDL (Figure 3C). Therefore, these data indicated that CG could suppress ox-LDL-induced foam cell formation in THP-1-derived macrophage.

CG Suppresses Ox-LDL-Induced Inflammation and Foam Cell Formation by Activating ATF-1

Previous studies demonstrated that ATF-1 confers atheroprotection in human monocyte-derived macrophages by regulating iron homeostasis and preventing foam cell formation.[11,15] Notably, ATF family members are established downstream effectors of flavonoids.[16,17] Given that CG is a bioactive flavonoid, we hypothesized that ATF-1 mediates CG's therapeutic effects against ox-LDL-triggered inflammatory responses and pathological foam cell accumulation. As shown in Figure 4A, CG promoted the phosphorylation of ATF-1, which has been demonstrated to be essential for the full functional activity of ATF-1.[11] The specific ATF-1 siRNAs were transfected into THP-1-derived macrophages

https://doi.org/10.2147/JIR.S516160

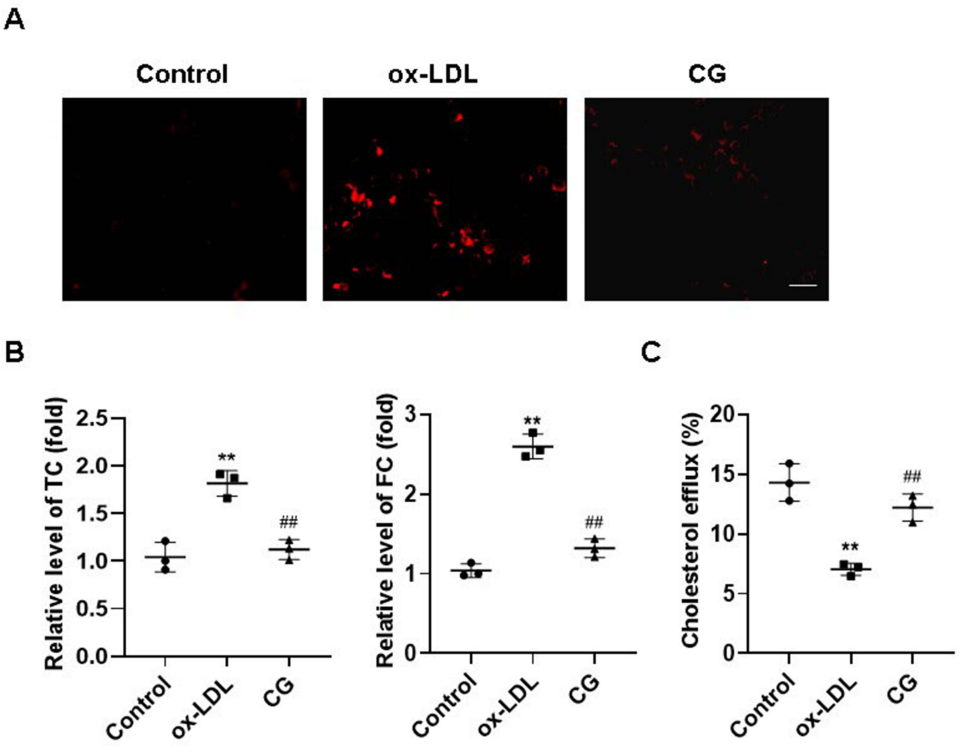

Figure 3 The effect of CG on ox-LDL-induced foam cell formation in THP-1-derived macrophages. THP-1-derived macrophages were incubated with CG for 24 h, prior to being stimulated with ox-LDL for 24 h. (**A**) The formation of foam cells in each group was determined using Nile red staining. Sacr bar=100μM. (**B**) The total cholesterol (TC) and free cholesterol (FC) were detected using their corresponding commercial kits, respectively. (**C**) Cellular cholesterol efflux was measured by counting cell-associated [^{3}H]-cholesterol using liquid scintillation counting method. **p<0.01 compared with control group; $^{\#\#}$p<0.01 compared with ox-LDL group.

(Figure 4B) to further validate the role of ATF-1 in the effects of CG on ox-LDL-induced inflammation and foam cell formation. The result showed that compared to control siRNA, ATF-1 siRNA significantly attenuated CG-induced decreases in the number of foam cells (Figure 4C) and the levels of TC and FC in ox-LDL-exposed THP-1-derived macrophages (Figure 4D). ATF-1 siRNA also increased the production of pro-inflammatory cytokines (TNF-α, IL-1β, and IL-6) and decreased the production of anti-inflammatory cytokines (IL-10) in ox-LDL-exposed THP-1-derived macrophages with CG treatment (Figure 4E). Moreover, CG treatment could reduce the expression levels of NLRP3 inflammasome-related proteins (NLRP3, ASC, and Caspase-1) in ox-LDL-expose THP-1-derived macrophages, while ATF-1 siRNA transfection ameliorated the decreases induced by CG (Figure 4F). Therefore, these results demonstrated that ATF-1 is involved in the inhibitory effects of CG on ox-LDL-induced inflammation and foam cell formation.

CG Activates ATF-1 to Suppress Foam Cell Formation by Inducing Liver X Receptor Beta

Previous studies have established that ATF-1 orchestrates the atheroprotective Mhem macrophage phenotype through transcriptional activation of Liver X receptor beta (LXR-β), triggers a cascade of cholesterol efflux-promoting genes, including LXR-α and ABCA1.[11] Therefore, we investigated whether ATF-1 mediates CG's anti-atherogenic effects by similarly upregulating LXR-β to inhibit foam cell formation. The results showed that CG treatment could increase the protein expression levels of LXR-β and its target gene, ABCA1, in ox-LDL-expose THP-1-derived macrophages, while ATF-1 siRNA transfection ameliorated the increases of these proteins induced by CG (Figure 5A). ATF-1 siRNA also reduced the mRNA level of LXR-β in CG-treated THP-1-derived macrophages (Figure 5B). Chromatin immunoprecipitation (ChIP) assay showed that binding of ATF-1 to the LXR-β enhancer was increased in THP-1-derived macrophages after CG treatment (Figure 5C). In addition, compared to control siRNA, LXR-β siRNA significantly increased in the number of

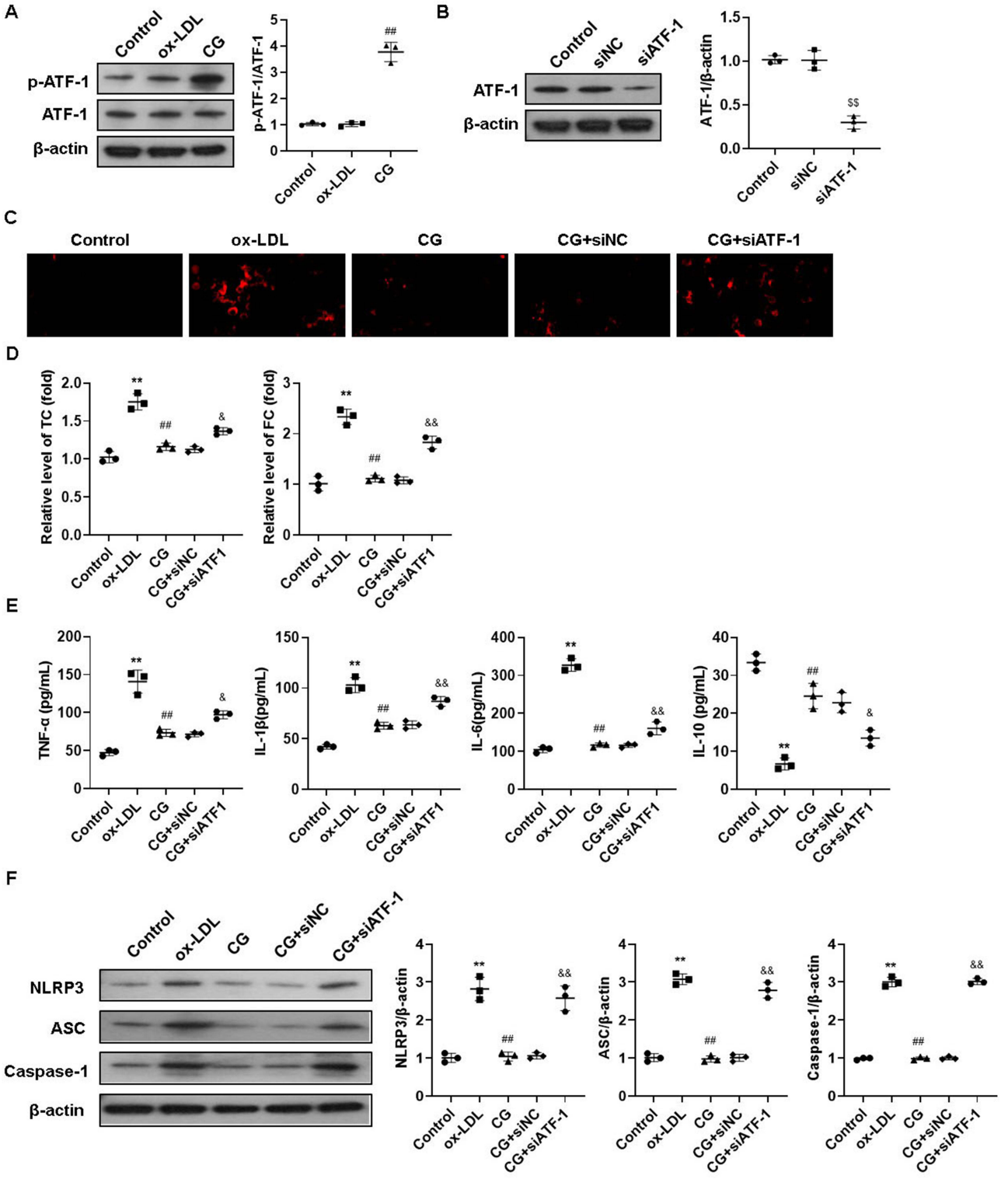

Figure 4 Activation of ATF-1 is involved in the inhibitory effect of CG on ox-LDL-induced foam cell formation and inflammation. (**A**) THP-1-derived macrophages were incubated with CG for 24 h, prior to being stimulated with ox-LDL for 24 h. The expression levels of ATF-1 and phosphorylated ATF-1 were detected by Western blotting. (**B**) THP-1-derived macrophages were transfected with negative control siRNA (siNC) and ATF-1 siRNA (siATF-1) for 24 h, and the expression levels of ATF-1 were detected by Western blotting. (**C**–**F**) THP-1-derived macrophages were transfected with siNC or siATF-1 for 24 h, the transfected cells were then incubated with CG for 24 h, prior to being stimulated with ox-LDL for 24 h. The formation of foam cells in each group was determined using Nile red staining, Sacr bar=100μM (**C**), the total cholesterol (TC) and free cholesterol (FC) were detected using their corresponding commercial kits, respectively (**D**), the production of inflammatory cytokines, including IL-6, IL-1β, TNF-α, and IL-10, was assayed by ELISA kits (**E**), the protein expressions of NLRP3, ASC, and caspase-1 were detected using Western blotting (**F**). $^{**}p<0.01$ compared with control group; $^{\#\#}p<0.01$ compared with ox-LDL group; $^{\$\$}p<0.01$ compared with siNC group; $^{\&}p<0.05$, $^{\&\&}p<0.01$ compared with CG + siNC group.

https://doi.org/10.2147/JIR.S516160

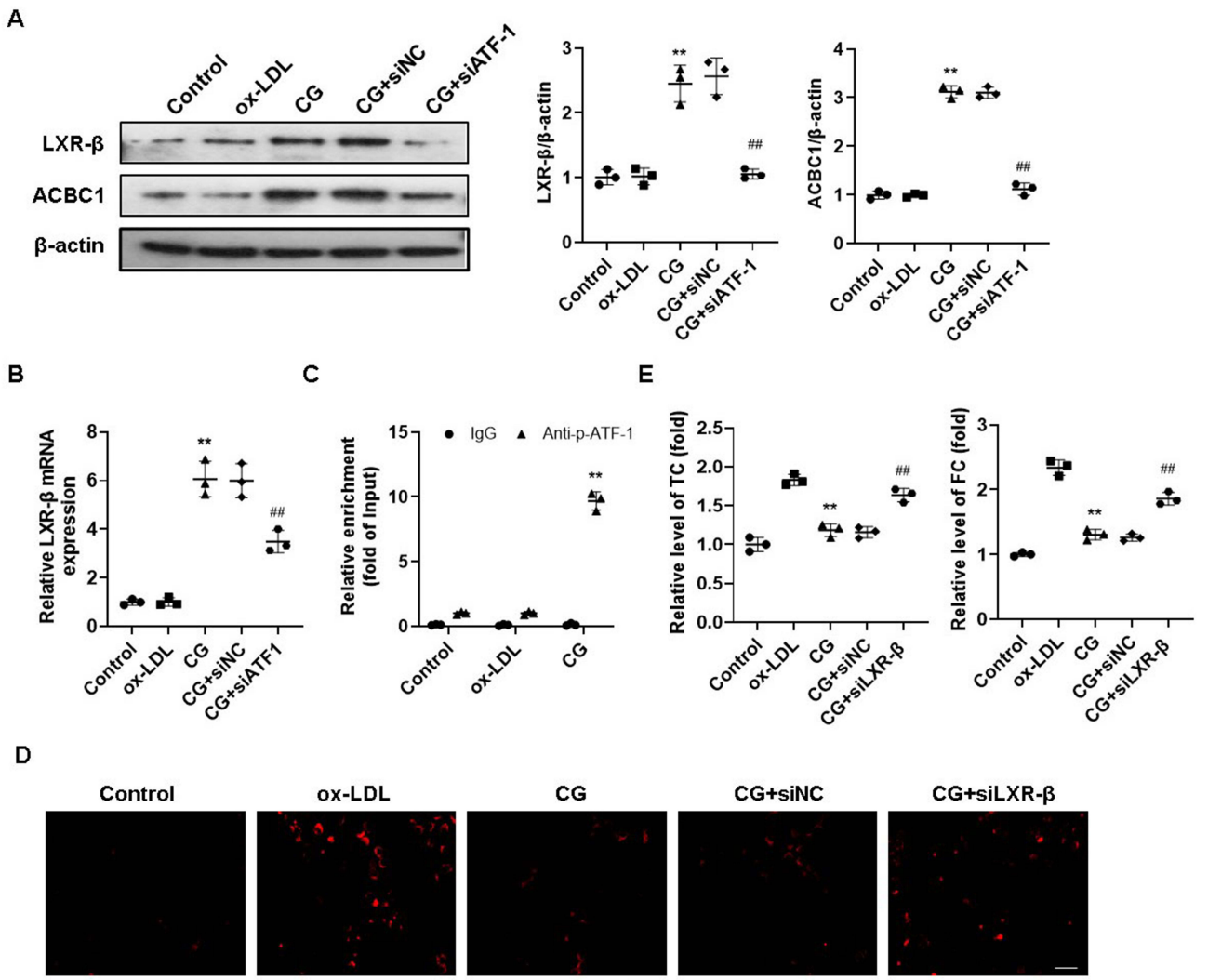

Figure 5 ATF-1 mediates CG-induced inhibition of foam cell formation by inducing Liver X receptor beta. (**A** and **B**) THP-1-derived macrophages were transfected with negative control siRNA (siNC) and ATF-1 siRNA (siATF-1) for 24 h, and the protein and mRNA levels of LXR-β were detected by Western blotting and qRT-PCR, respectively. (**C**) Chromatin immunoprecipitation (ChIP) analysis of CG-treated THP-1-derived macrophages using anti–p-ATF-1. (**D** and **E**) THP-1-derived macrophages were transfected with control siRNA (siNC) and LXR-β siRNA (siLXR-β) for 24 h, the transfected cells were then incubated with CG for 24 h, prior to being stimulated with ox-LDL for 24 h. The formation of foam cells in each group was determined using Nile red staining, Sacr bar=100μM (**D**), the total cholesterol (TC) and free cholesterol (FC) were detected using their corresponding commercial kits, respectively (**E**). **p<0.01 compared with ox-LDL group; ##p<0.01 compared with CG + siNC group.

foam cells (Figure 5D) and the levels of TC and FC in CG-treated THP-1-derived macrophages (Figure 5E). Therefore, these results suggested that CG activates ATF-1 to suppress foam cell formation by inducing LXR-β.

CG Activates ATF-1 to Suppress Inflammation by Inducing CFTR

To investigate the mechanism by which ATF-1 mediates CG-induced inhibition of inflammation in ox-LDL-expose THP-1-derived macrophages, we first detected the expression level of cystic fibrosis transmembrane conductance regulator (CFTR) in the ATF-1 siRNA transfected THP-1-derived macrophages because ATF-1 has been demonstrated to be the transcription factor of CFTR,[18] which was shown to protect vascular inflammation and AS in apolipoprotein E-deficient mice.[19] Western blot analysis revealed that ATF-1 siRNA obviously reduced CFTR expression in CG-treated THP-1-derived macrophages (Figure 6A). ATF-1 siRNA also reduced the mRNA level of CFTR in CG-treated THP-1-derived macrophages (Figure 6B). ChIP assay showed that CG treatment promotes the binding of ATF-1 to the promoter of CFTR (Figure 6C). To explore the role of CFTR in CG-induced inhibition of inflammation, we then examined the

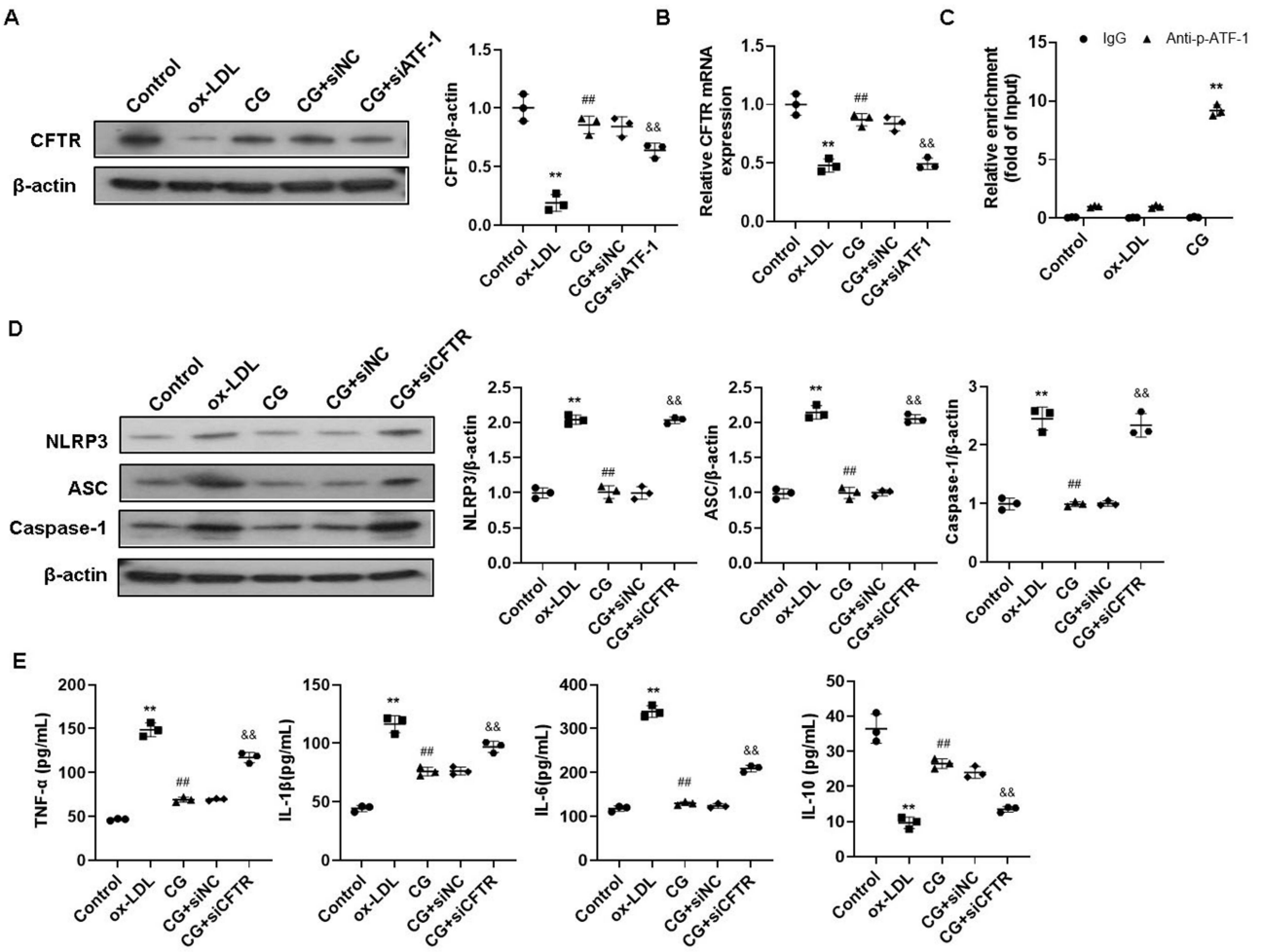

Figure 6 ATF-1 mediates CG-induced inhibition of inflammation by inducing CFTR. (**A** and **B**) THP-1-derived macrophages were transfected with negative control siRNA (siNC) and ATF-1 siRNA (siATF-1) for 24 h, and the protein and mRNA levels of cystic fibrosis transmembrane conductance regulator (CFTR) were detected by Western blotting and RT-qPCR, respectively. (**C**) Chromatin immunoprecipitation (ChIP) analysis of CG-treated THP-1-derived macrophages using anti–p-ATF-1. (**D** and **E**) THP-1-derived macrophages were transfected with control siRNA (siNC) and CFTR siRNA (siCFTR) for 24 h, the transfected cells were then incubated with CG for 24 h, prior to being stimulated with ox-LDL for 24 h. The protein expressions of NLRP3, ASC, and caspase-1 were detected using Western blotting (**D**), the production of inflammatory cytokines, including IL-6, IL-1β, TNF-α, and IL-10, was assayed by ELISA kits (**E**). **p<0.01 compared with control group; ##p<0.01 compared with ox-LDL group; &&p<0.01 compared with CG + siNC group.

expression levels of pro-inflammatory proteins and cytokines in CG-treated THP-1-derived macrophages, in the presence of CFTR siRNA. Figure 6D demonstrated that CFTR siRNA significantly deteriorated the CG-induced decreases in the levels of NLRP3, ASC, and caspase-1 in the ox-LDL-exposed THP-1-derived macrophages. The CG-induced decreases in the levels of IL-6, IL-1β, TNF-α, and increases in the levels of IL-10 were also reserved by CFTR siRNA (Figure 6E). Therefore, these data suggested that CG activates ATF-1 to suppress inflammation by inducing CFTR.

Activation of p38/MAPK Pathway Is Required for CG-Induced Phosphorylation of ATF-1 and Inhibition of Foam Cell Formation and Inflammation in Ox-LDL-Expose THP-1-Derived Macrophages

Previous studies showed that the activation of ATF-1 was modulated by specific kinase in different types of cells or in the same cells under different stresses, such as p38,[20,21] AKT,[22,23] JNK,[24] and ERK1/2.[25] Therefore, we determined which of these kinases was responsible for ATF-1 activation induced by CG in ox-LDL-exposed THP-1-derived macrophages. As shown in Figure 7A, the phosphorylation levels of AKT and P38 were obviously upregulated after CG treatment, while the phosphorylation levels of the other kinases (ERK and JNK) remained unchanged. THP-1-derived macrophages

https://doi.org/10.2147/JIR.S516160

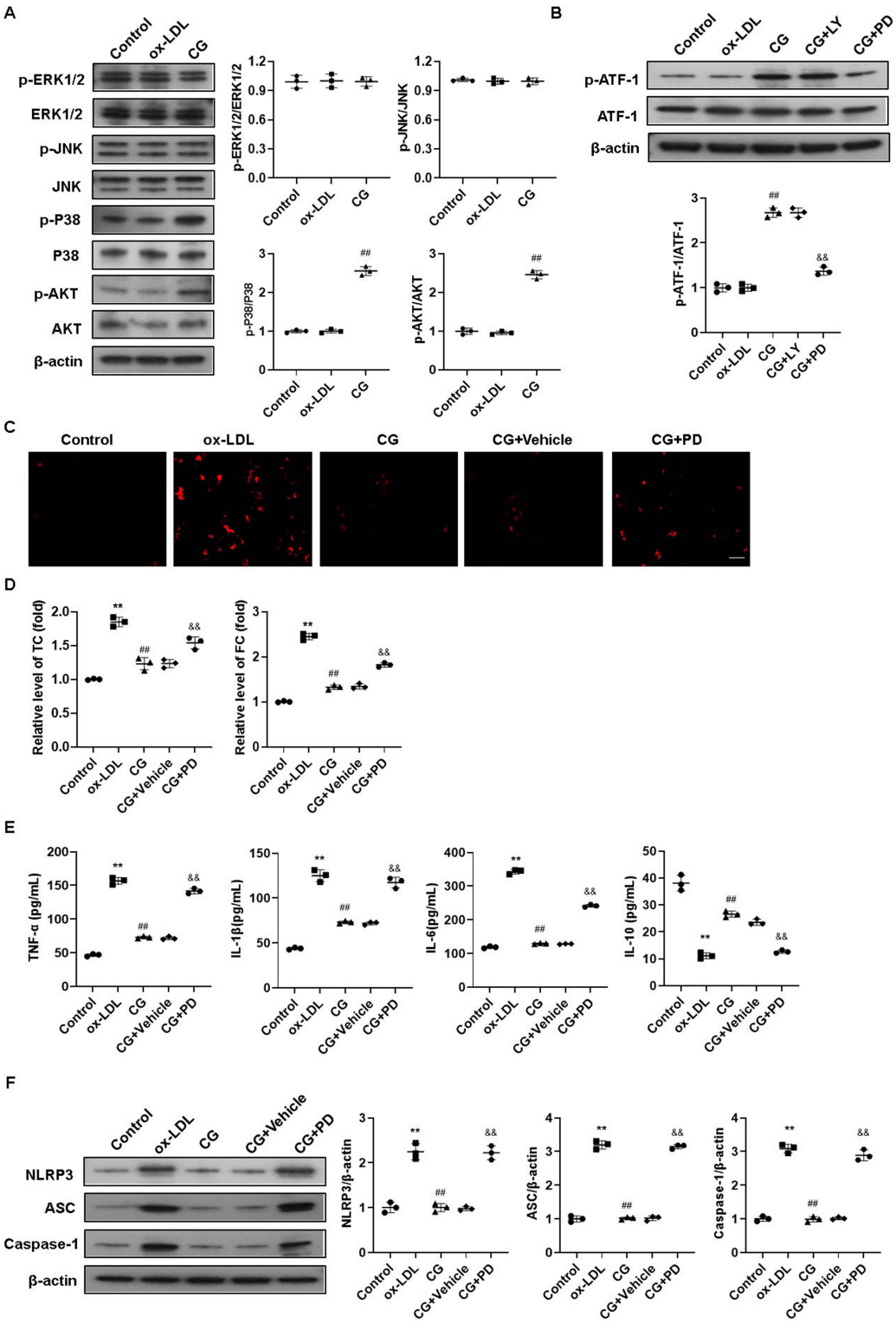

Figure 7 Activation of p38/MAPK is involved in CG-induced phosphorylation of ATF-1 and inhibition of foam cell formation and inflammation in ox-LDL-expose THP-1-derived macrophages. (**A**) THP-1-derived macrophages were incubated with CG for 24 h, prior to being stimulated with ox-LDL for 24 h. The expression levels of phosphorylated p38, AKT, JNK, and ERK1/2 were detected by Western blotting. (**B**) THP-1-derived macrophages were treated with LY294002 or PD169316 for 12 h, the treated cells were then incubated with CG for 24 h, prior to being stimulated with ox-LDL for 24 h. The expression levels of phosphorylated ATF-1, p38 and AKT were detected by Western blotting. (**C**–**F**) THP-1-derived macrophages were treated with PD169316 for 12 h, the treated cells were then incubated with CG for 24 h, prior to being stimulated with ox-LDL for 24 h. The formation of foam cells in each group was determined using Nile red staining, Sacr bar=100μM (**C**), the total cholesterol (TC) and free cholesterol (FC) were detected using their corresponding commercial kits, respectively (**D**), the production of inflammatory cytokines, including IL-6, IL-1β, TNF-α, and IL-10, was assayed by ELISA kits (**E**), the protein expressions of NLRP3, ASC, and Caspase-1 were detected using Western blotting (**F**). **p<0.01 compared with control group; ##p<0.01 compared with ox-LDL group; &&p<0.01 compared with CG group.

treated with the AKT inhibitor, LY294002, showed no effect on ATF-1 activation under CG treatment (Figure 7B). However, the P38 inhibitor, PD169316, obviously abolished ATF-1 activation in CG-treated THP-1-derived macrophages (Figure 7B), suggesting that p38 mediates CG-induced ATF-1 activation in ox-LDL-exposed THP-1-derived macrophages.

The involvement of p38 in CG-induced inhibition of foam cell formation and inflammation were then investigated. The result showed that PD169316 significantly increased in the number of foam cells (Figure 7C) and the levels of TC and FC in ox-CG-exposed THP-1-derived macrophages (Figure 7D). PD169316 also increased the production of pro-inflammatory cytokines (TNF-α, IL-1β, and IL-6), decreased the anti-inflammatory cytokines (IL-10) (Figure 7E), and increased the expression levels of NLRP3 inflammasome-related proteins (NLRP3, ASC, and Caspase-1) in CG-exposed THP-1-derived macrophages (Figure 7F). Thus, our results confirmed the involvement of p38 MAPK in CG-induced inhibition of foam cell formation and inflammation in ox-LDL-exposed THP-1-derived macrophages.

Discussion

Despite the growing interest in natural compounds for AS treatment, the therapeutic potential of CG remains largely unexplored. Our study provides the experimental evidence that CG significantly suppresses oxLDL-induced foam cell formation and inflammatory responses in THP-1-derived macrophages. Building on this discovery, we systematically elucidated the underlying molecular mechanisms, revealing CG's multi-target action through key signaling pathways.

ATF-1 is a multifunctional transcription factor implicated in development, tumorigenesis, and immune regulation.[7,8] Notably, Boyle et al[11] demonstrated that ATF-1 drives human plaque monocytes to adopt an atheroprotective macrophage phenotype (Mhem), distinct from classical M1, M2, or Mox subsets. This protective effect was mediated through ATF-1-dependent upregulation of LXR-β, which in turn activated cholesterol efflux genes, including ABCA1 and LXR-α. Critically, ATF-1 phosphorylation was essential for its functional activity, highlighting its therapeutic potential in AS by counteracting foam cell formation. Our results showed that in oxLDL-exposed THP-1-derived macrophages, CG significantly enhanced ATF-1 phosphorylation, mirroring the atheroprotective pathway reported by Boyle et al.[11] ATF-1 knockdown abolished CG's inhibition of foam cell formation, confirming ATF-1 as a non-redundant mediator of CG's effects. These results align with prior work, extending ATF-1's protective role to CG-treated macrophages and underscoring its broader therapeutic relevance in AS.

We next explored the potential downstream effector of ATF-1 in mediating CG-induced inhibition of inflammation. CFTR is an anion channel in the apical membrane of epithelial cells. Dysfunction of the CFTR protein has been demonstrated to be associated with multiorgan dysfunction.[26] Emerging studies has suggested that CFTR protein is not just a chloride channel, it also regulates numerous other pathways, such as immune cells, glutathione and thiocyanate, and the metabolism of lipids.[27] CFTR has been shown to protect against vascular inflammation and AS in apolipoprotein E-deficient mice.[19] Importantly, ATF-1 was shown to enhance CFTR transcription through the Y-box element.[18] Our data showed that silencing of ATF-1 by siRNA obviously prevented CG-induced upregulation of CFTR. CG enhanced the binding of ATF-1 to the promoter of CFTR. CFTR siRNA attenuated CG-induced inhibition of inflammation. These results suggest that ATF-1 mediates CG-induced inhibition of inflammation by upregulating CFTR via directly binding to its promoter in oxLDL-exposed THP-1-derived macrophages. A previous study showed that CFTR prevented inflammation and AS via inhibition of NFκB,[19] which plays a key role in oxLDL-induced formation of foam cells and expression of inflammatory molecules.[28,29] Therefore, it will be worthwhile to investigate whether CFTR mediates CG-induced inhibition of inflammation via inhibition of NFκB in oxLDL-exposed THP-1-derived macrophages.

To elucidate the upstream regulators of ATF-1 activation in CG-treated THP-1-derived macrophages, we focused on kinases previously implicated in ATF-1 phosphorylation, including p38 MAPK,[20,21] AKT,[22,23] JNK,[24] and ERK1/2.[25] Given that ATF-1 activation is context-dependent, varying by cell type and stress conditions, we sought to identify the macrophage-specific kinase(s) responsible for CG-induced ATF-1 activation. Among all reported ATF-1-activating kinases, we found that only p38 MAPK and AKT exhibited increased phosphorylation following CG treatment. Pharmacological inhibition of p38 MAPK, but not AKT, abolished CG-induced ATF-1 activation. p38 MAPK inhibition also reversed CG's anti-atherogenic effects, attenuating its suppression of foam cell formation and inflammatory

responses in oxLDL-exposed macrophages. These results establish p38 MAPK as the dominant kinase mediating CG's effects via ATF-1 activation. The p38 MAPK/ATF-1 axis thus represents a critical pathway for CG's inhibition of foam cell formation and inflammation in THP-1-derived macrophages. While our findings highlight p38 MAPK's role in this model, its cell type–specificity warrants caution. Further studies are needed to determine whether the p38 MAPK/ATF-1 mechanism extends to other macrophage subtypes, such as primary human macrophages and polarized M1/M2 phenotypes.

Emerging evidence has identified multiple signaling pathways as downstream targets of CG. Chen et al recently demonstrated that CG promotes diabetic wound healing by recruiting anti-inflammatory monocytes and modulating macrophage polarization toward the M2 phenotype through the ROS/AMPK/STAT6 pathway, while simultaneously reducing mitochondrial glycolysis rates.[30] As a principal bioactive component of Buyang Huanwu decoction, CG has been shown to exert protective effects against diabetes-associated complications by attenuating diabetes-accelerated AS by inhibiting excessive mitochondrial fission via the AMPK/Drp1 pathway;[6] and ameliorating renal inflammation and fibrosis in diabetic nephropathy through suppression of both TGF-β1/Smad3 and NF-κB signaling pathways in mesangial cells.[31] Notably, these pathways (AMPK, TGF-β1/Smad3, and NF-κB) all play pivotal roles in AS pathogenesis.[32–34] While our current study identified the p38 MAPK/ATF-1 signaling axis as a key mediator, future investigations should explore whether these additional pathways contribute to CG-induced M2 macrophage polarization and its consequent anti-atherosclerotic effects.

The findings of this study demonstrate significant translational potential for CG, particularly in light of increasing pharmacological interest in natural compounds. CG has demonstrated promising bioactivities, including anti-inflammatory, antioxidant, and cardioprotective effects, suggesting its therapeutic utility in conditions such as cardiovascular diseases, diabetic complications, and neurodegenerative disorders. However, its clinical translation faces challenges, primarily due to poor oral bioavailability resulting from low solubility, intestinal metabolism, and rapid systemic clearance. To address these limitations, advanced formulation strategies could be employed. For instance, nanocarrier systems or phospholipid complexes may enhance CG's solubility and intestinal absorption. These advanced delivery systems could significantly improve CG's pharmacokinetic profile while maintaining its therapeutic efficacy, potentially enabling its transition from preclinical studies to clinical applications. Future research should focus on optimizing these delivery platforms while evaluating their safety and efficacy in relevant disease models.

While this study provides valuable insights into the mechanisms underlying CG's anti-atherosclerotic effects, several limitations should be acknowledged. First, the findings were primarily validated using in vitro cell models, and further in vivo studies are necessary to confirm the anti-atherosclerotic efficacy of CG. Second, this study focused exclusively on THP-1-derived macrophages, leaving the effects of CG on other macrophage subtypes unexplored, such as primary human macrophages and polarized M1/M2 phenotype. Future studies should expand their scope to investigate the impact of CG on these subtypes, which would provide a more comprehensive understanding of its therapeutic potential against AS. Third, although our study highlights the role of the p38/ATF-1 pathway, it is likely that additional molecular mechanisms contribute to CG's modulation of macrophage-related AS pathogenesis. These unexplored mechanisms represent a promising avenue for future research.

Conclusion

In conclusion, our findings demonstrate that CG attenuates foam cell formation and inflammation in ox-LDL-exposed THP-1-derived macrophages by activating p38 MAPK signaling, which phosphorylates ATF-1 and subsequently upregulates LXR-β and CFTR expression. Although the anti-atherosclerotic effects and mechanisms of CG identified in this study require further validation through in vivo studies, our results provide novel mechanistic insights into the macrophage-centric therapeutic potential of CG. These findings underscore the promise of CG as a therapeutic agent for AS. Future studies should prioritize in vivo validation and clinical translation to fully elucidate and harness its therapeutic potential.

Abbreviations

AS, atherosclerosis; CG, flavonoid calycosin-7-glucoside; PMA, phorbol-12-myristate-13-acetate; ATF-1, activating transcription factor-1; LXR-β, liver X receptor beta; CFTR, cystic fibrosis transmembrane conductance regulator; DMY, dihydromyricetin; NOB, Nobiletin; AM, Astragalus membranaceus; TC, total cholesterol; FC, free cholesterol.

Data Sharing Statement

The data is available upon request from the correspondence author, Yaohong Song.

Funding

Fundings for this research were provided by Nanjing Youth Talent Training Program for Traditional Chinese Medicine (ZYQ20009), Nanjing Health Science and Technology Development Special Fund Project for 2024 (YKK24171), Nanjing University of Chinese Medicine Natural Science Foundation Project of 2023(XZR2023061), and Song Yaohong Nanjing Famous Chinese Medicine Practitioner's Studio (2023-NJSMZYGZS-SYH).

Disclosure

The authors declare that there are no competing interests in this work.

References

1. Tasouli-Drakou V, Ogurek I, Shaikh T, Ringor M, DiCaro MV, Lei K. Atherosclerosis: a Comprehensive Review of Molecular Factors and Mechanisms. *Int J mol Sci*. 2025;26(3):1364. doi:10.3390/ijms26031364
2. Zhang L, Li J, Kou Y, et al. Mechanisms and treatment of atherosclerosis: focus on macrophages. *Front Immunol*. 2024;15:1490387. doi:10.3389/fimmu.2024.1490387
3. Xiao L, Zhao M, Linghu KG, et al. Ganweikang extract protects hepatocytes from oxidative injury by activating Nrf2/HO-1 and MAPKs pathways. *Fitoterapia*. 2024;178:106146. doi:10.1016/j.fitote.2024.106146
4. Wei X, Zeng Y, Meng F, et al. Calycosin-7-glucoside promotes mitochondria-mediated apoptosis in hepatocellular carcinoma by targeting thioredoxin 1 to regulate oxidative stress. *Chem Biol Interact*. 2023;374:110411. doi:10.1016/j.cbi.2023.110411
5. Wang PC, Wang SX, Yan XL, et al. Combination of paeoniflorin and calycosin-7-glucoside alleviates ischaemic stroke injury via the PI3K/AKT signalling pathway. *Pharm Biol*. 2022;60(1):1469–1477. doi:10.1080/13880209.2022.2102656
6. Tong W, Leng L, Wang Y, et al. Buyang huanwu decoction inhibits diabetes-accelerated atherosclerosis via reduction of AMPK-Drp1-mitochondrial fission axis. *J Ethnopharmacol*. 2023;312:116432. doi:10.1016/j.jep.2023.116432
7. Tellez C, Jean D, Bar-Eli M. Construction and expression of intracellular anti-ATF-1 single chain Fv fragment: a modality to inhibit melanoma tumor growth and metastasis. *Methods*. 2004;34(2):233–239. doi:10.1016/j.ymeth.2004.03.016
8. Chelakkot VS, Thomas K, Romigh T, et al. MC1R signaling through the cAMP-CREB/ATF-1 and ERK-NFkappaB pathways accelerates G1/S transition promoting breast cancer progression. *NPJ Precis Oncol*. 2023;7(1):85. doi:10.1038/s41698-023-00437-1
9. Zhao L, Xia W, Jiang P. CREB1 and ATF1 Negatively Regulate Glutathione Biosynthesis Sensitizing Cells to Oxidative Stress. *Front Cell Dev Biol*. 2021;9:698264. doi:10.3389/fcell.2021.698264
10. Shi F, He R, Zhu J, Lu T, Zhong L. miR-589-3p promoted osteogenic differentiation of periodontal ligament stem cells through targeting ATF1. *J Orthop Surg Res*. 2022;17(1):221. doi:10.1186/s13018-022-03000-z
11. Boyle JJ, Johns M, Kampfer T, et al. Activating transcription factor 1 directs Mhem atheroprotective macrophages through coordinated iron handling and foam cell protection. *Circ Res*. 2012;110(1):20–33. doi:10.1161/CIRCRESAHA.111.247577
12. Reustle A, Torzewski M. Role of p38 MAPK in Atherosclerosis and Aortic Valve Sclerosis. *Int J mol Sci*. 2018;19(12):3761. doi:10.3390/ijms19123761
13. Tan KS, Nackley AG, Satterfield K, Maixner W, Diatchenko L, Flood PM. Beta2 adrenergic receptor activation stimulates pro-inflammatory cytokine production in macrophages via PKA- and NF-kappaB-independent mechanisms. *Cell Signal*. 2007;19(2):251–260. doi:10.1016/j.cellsig.2006.06.007
14. Chen R, Yang M. Melatonin Inhibits OGD/R-Induced H9c2 Cardiomyocyte Pyroptosis via Regulation of MT2/miR-155/FOXO3a/ARC Axis. *Int Heart J*. 2022;63(2):327–337. doi:10.1536/ihj.21-571
15. Wan X, Huo Y, Johns M, et al. 5'-AMP-activated protein kinase-activating transcription factor 1 cascade modulates human monocyte-derived macrophages to atheroprotective functions in response to heme or metformin. *Arterioscler Thromb Vasc Biol*. 2013;33(11):2470–2480. doi:10.1161/ATVBAHA.113.300986
16. Tang F, Xu Y, Gao E, et al. Amentoflavone attenuates cell proliferation and induces ferroptosis in human gastric cancer by miR-496/ATF2 axis. *Chem Biol Drug Des*. 2023;102(4):782–792. doi:10.1111/cbdd.14288
17. Liu L, Liu T, Tao W, et al. Flavonoids from Scutellaria barbata D. Don exert antitumor activity in colorectal cancer through inhibited autophagy and promoted apoptosis via ATF4/sestrin2 pathway. *Phytomedicine*. 2022;99:154007. doi:10.1016/j.phymed.2022.154007
18. Li S, Moy L, Pittman N, et al. Transcriptional repression of the cystic fibrosis transmembrane conductance regulator gene, mediated by CCAAT displacement protein/cut homolog, is associated with histone deacetylation. *J Biol Chem*. 1999;274(12):7803–7815. doi:10.1074/jbc.274.12.7803
19. Li Z, Shen Z, Xue H, et al. CFTR protects against vascular inflammation and atherogenesis in apolipoprotein E-deficient mice. *Biosci Rep*. 2017;37(4):680. doi:10.1042/BSR20170680.

20. Rikitake Y, Hirata K, Kawashima S, et al. Signaling mechanism underlying COX-2 induction by lysophosphatidylcholine. *Biochem Biophys Res Commun*. 2001;281(5):1291–1297. doi:10.1006/bbrc.2001.4510
21. Tan Y, Rouse J, Zhang A, Cariati S, Cohen P, Comb MJ. FGF and stress regulate CREB and ATF-1 via a pathway involving p38 MAP kinase and MAPKAP kinase-2. *EMBO J*. 1996;15(17):4629–4642. doi:10.1002/j.1460-2075.1996.tb00840.x
22. Rossi SP, Windschuttl S, Matzkin ME, et al. Reactive oxygen species (ROS) production triggered by prostaglandin D2 (PGD2) regulates lactate dehydrogenase (LDH) expression/activity in TM4 Sertoli cells. *mol Cell Endocrinol*. 2016;434:154–165. doi:10.1016/j.mce.2016.06.021
23. Bose S, Kim S, Oh Y, Moniruzzaman M, Lee G, Cho J. Effect of CCL2 on BV2 microglial cell migration: involvement of probable signaling pathways. *Cytokine*. 2016;81:39–49. doi:10.1016/j.cyto.2016.02.001
24. Liu B, Yu J, Taylor L, Zhou X, Polgar P. Microarray and phosphokinase screenings leading to studies on ERK and JNK regulation of connective tissue growth factor expression by angiotensin II 1a and bradykinin B2 receptors in Rat1 fibroblasts. *J Cell Biochem*. 2006;97(5):1104–1120. doi:10.1002/jcb.20709
25. Martin MJ, Calvo N, de Boland AR, Gentili C. Molecular mechanisms associated with PTHrP-induced proliferation of colon cancer cells. *J Cell Biochem*. 2014;115(12):2133–2145. doi:10.1002/jcb.24890
26. Ong T, Ramsey BW. Cystic Fibrosis: a Review. *JAMA*. 2023;329(21):1859–1871. doi:10.1001/jama.2023.8120
27. Hanssens LS, Duchateau J, Casimir GJ. CFTR Protein: not Just a Chloride Channel? *Cells*. 2021;10(11):2844. doi:10.3390/cells10112844
28. Chang S, Zhang G, Li L, et al. Sirt4 deficiency promotes the development of atherosclerosis by activating the NF-kappaB/IkappaB/CXCL2/3 pathway. *Atherosclerosis*. 2023;373:29–37. doi:10.1016/j.atherosclerosis.2023.04.006
29. Karunakaran D, Nguyen MA, Geoffrion M, et al. RIPK1 Expression Associates With Inflammation in Early Atherosclerosis in Humans and Can Be Therapeutically Silenced to Reduce NF-kappaB Activation and Atherogenesis in Mice. *Circulation*. 2021;143(2):163–177. doi:10.1161/CIRCULATIONAHA.118.038379
30. Chen J, Ma H, Meng Y, et al. Analysis of the mechanism underlying diabetic wound healing acceleration by Calycosin-7-glycoside using network pharmacology and molecular docking. *Phytomedicine*. 2023;114:154773. doi:10.1016/j.phymed.2023.154773
31. Wu W, Wang Y, Li H, Chen H, Shen J. Buyang Huanwu Decoction protects against STZ-induced diabetic nephropathy by inhibiting TGF-beta/Smad3 signaling-mediated renal fibrosis and inflammation. *Chin Med*. 2021;16(1):118. doi:10.1186/s13020-021-00531-1
32. Wada T, Senokuchi T, Shi Y, et al. Orally administrated acetate inhibits atherosclerosis progression through AMPK activation via GPR43 in plaque macrophages. *Atherosclerosis*. 2025;401:119088. doi:10.1016/j.atherosclerosis.2024.119088
33. He Z, Xue H, Liu P, et al. miR-4286/TGF-beta1/Smad3-Negative Feedback Loop Ameliorated Vascular Endothelial Cell Damage by Attenuating Apoptosis and Inflammatory Response. *J Cardiovasc Pharmacol*. 2020;75(5):446–454. doi:10.1097/FJC.0000000000000813
34. Fan X, Han J, Zhong L, et al. Macrophage-Derived GSDMD Plays an Essential Role in Atherosclerosis and Cross Talk Between Macrophages via the Mitochondria-STING-IRF3/NF-kappaB Axis. *Arterioscler Thromb Vasc Biol*. 2024;44(6):1365–1378. doi:10.1161/ATVBAHA.123.320612